'93 KACC (1993.10.20~22)

Modeling and Experiment for the Force/Impact Control via Passive Hardware Damper

°Y.H. Oh, W.K. Chung and Y. Youm
Robotics Lab. Department of Mechanical Engineering, POSTECH,
P.O. Box 125, Pohang, Kyungbuk, 170-600, KOREA

Abstract: This paper deals with the modeling and experiment of a robot system for force/impact control performance. The basic model is composed of a direct drive motor, servo amplifier, link, force sensor and environments. Based on the developed model, the stability of the whole system was analyzed via root locus method. For the force control, integral force compensation with velocity feedback method shows the best performance of all the explicit force control strategies. In dealing with impact, PID position control and the explicit force control method were implemented. Instead of add more damping to the robot system by velocity feedback, we developed a new passive damping method and it was also applied to enhance the damping characteristic of the system.

1 Introduction

As the tasks of robot arms expand to jobs which require contact with environment, the capability to cope with a situation involving force and impact becomes necessary. The force control strategies developed so far are based on the assumption that the robot maintains stable contact initially. In real situation, however, the contact period is inevitable to do some tasks and stable contact during the transient period determine the success of the force control thereafter. The impact will affect the performance of the developed force controller seriously and thus the force and impact control issues should be handled simultaneously to perform the desired task successfully. The simple idea to resolve the impact problem is to give damping characteristic to the system to reduce the rebounce after the initial collision [5] and to ensure the stable contact like the human knee joint.

The force control issue has been studied widely and can be categorized as the impedance control and the explicit force control. In the impedance control [4], a relation between force and position is given in terms of the target dynamics to perform a task. The switching of the control modes between position and force is not necessary. However it requires exact model of the robot and knowledge of environment position and thus it is difficult to specify the desired force. In contrast with the impedance control, the explicit force control method requires the switching of control modes but the desired force can be easily specified. Among the various force control methods, the integral force control method shows better performance with respect to the contact discontinuity and steady state error [6, 1, 2]. For the impact control problem, some of researchers studied the modeling of force controlled system[7] and the effects of collision[8] recently. In dealing with impact, however, many researchers have used the software damping method to prevent the rebounding and improve the system stability. But, when one tries to implement the velocity feedback[1] during the impact, the noise signal usually deteriorates and restricts the performance of the controller.

In this paper, we propose a passive hardware damping method originated from the human knee joint where the meniscus and the synovial fluid between the articular cartilage provide inherent damping to the knee joint when there is an impact from the foot. The main goal of this study is to make stable contact as fast as possible without rebounding and to track the desired force after the contact based on the stability analysis of the whole system. In section 2, we will derive the dynamic model of our system including the passive damper and the simulations and analyses are conducted in section 3 for the model. Experimental results for force/impact control are addressed in section 4 and the conclusions will be made in the final section.

2 Modeling of the System

The system we are dealing with is composed of 1-DOF direct drive robotic arm, passive damper and environment. Fig. 1 shows the schematic diagram of the system. To analyze the stability of the system, and to understand the effect of passive damper on the system performance, the dynamic model of the system is required. The proposed linearized model of the system is shown in Fig. 2, where f_a denotes the applied input force at the tip of arm

[1] Hereafter velocity feedback and active damping will be used interchangeably.

and it is expressed as:

$$f_a = \frac{\tau_a}{l_a} , \tag{1}$$

where l_a is the arm length and τ_a is the applied joint torque. The X_1 can be approximated by the following:

$$X_1 \approx l_a \theta_m , \tag{2}$$

where θ_m is the joint position. K_e is the stiffness of the environment and C_e is the damping coefficient of the environment. $C_{D/A}$ denotes the equivalent passive damping/active damping value at the tip of arm. The subscript 's' denotes the parameters of force sensor. The values of basic dynamic parameters of the system were obtained from simulations and preliminary experiments [9].

2.1 Force Sensor/Amplifier and Contact Force

A strain-gauge type of force sensor with maximum capability of 100kgf and its amplifier were used to measure the compression force at the tip of the arm. When the arm contacts with environment, the reaction force f_R is considered as follows by neglecting the inertial force:

$$\begin{aligned} f_R &= [K_s(X_2 - X_e) + C_s(\dot{X}_2 - \dot{X}_e)] \times \\ &\quad 1[K_s(X_2 - X_e) + C_s(\dot{X}_2 - \dot{X}_e)] , \end{aligned} \tag{3}$$

where X_2 is the tip position of the arm and X_e is the position of the environment. To consider contact/noncontact condition the *unit-step function* $1(\cdot)$ is used. In contact case, the measured force f_m is assumed as follows:

$$f_m = K_s(X_2 - X_e) , \tag{4}$$

The sensor amplifier has time-delay characteristic and thus it is modeled as a time-delay system. To construct the linear model, the amplifier model is linearized by the bilinear approximation as follows:

$$G_{amp}(s) = e^{-T_d s} \approx \frac{1 - T_d/2}{1 + T_d/2} , \tag{5}$$

where T_d is delay time, which was identified from simulations.

The resulting combined dynamic model of the force sensor/amplifier can be represented as follows:

$$\frac{f_m(s)}{f_R(s)} = \left(\frac{1 - \frac{T_d}{2}s}{1 + \frac{T_d}{2}s}\right)\frac{K_s}{C_s s + K_s} . \tag{6}$$

2.2 Driving System, Arm and Environments

An amplifier of the motor produces a output current for a given input voltage. In reality, the current amplifier and motor have a finite bandwidth and thus the driving system can be modeled as follows:

$$\frac{\tau_a(s)}{V_c(s)} = \frac{K}{T_c s + 1} , \tag{7}$$

where $V_c(s)$ is commanded voltage, $\tau_a(s)$ is motor torque generated actually. In computing τ_a, the following relation was used

$$\tau_a = l_a \times f_m , \tag{8}$$

where f_m is the measured force at the tip of the arm. In Eqn. (7), K is the constant which is product of servo amplifier DC gain and motor torque constant. T_c is time constant of the servo amplifier, which was computed from the manual.

In force control mode, the arm can not be treated as a rigid-body, especially when it contacts with a very stiff environment. We consider the link itself as a kinematic constraint which has no mass property. The arm is then assumed to has a concentrated lumped-mass at the endpoint of the arm and it is partioned into the collocated mass (M_1) and noncollocated mass (M_2) to consider the structural dynamics of the arm. Stiffness (K_a) and damping coefficient (C_a) are inserted between M_1 and M_2.

We use two different environments: a steel ingot and a rubber plate. The steel ingot can be considered as the rigid-body. The rubber plate is assumed as the first order impedance model-that is K_r and C_r and these can be expressed as follows:

$$f_R = C_r \dot{X}_e + K_r X_e . \tag{9}$$

2.3 Passive Damper

To add more damping to the system, we developed a new passive damper. The passive damper [10] is composed of a solenoid valve and a rotary vane and it is attached to the joint axis of the motor. The schematics of the passive damper is shown in Fig. 3(a). The damping coefficient can be changed by varying the clearance between the vane and cylinder. The switching of On/Off control mode is made depending on the magnitude of the measured force at the tip of the arm. If the magnitude of measured force is below the threshold value, the solenoid valve is in 'Off' state. In this case, the rotary vane can rotate at both directions about the joint axis freely. When the measured force is above the threshold value, the valve is 'On' state which means that only the unidirectional flow is allowed through the valve. The rotary vane can only move to one direction and if the joint tries to move backward, it experiences extremely large damping characteristic due to the solenoid valve. For simplicity, we model the damper as coulomb and viscous frictions. Ideal characteristic of the passive damper can be depicted in Fig. 3(b) and we will use this characteristic in impact control to reduce the rebounce when the robot collides with the environment.

3 Controller Design and Analysis

Assuming that the model is accurate, the stability analysis and simulations were performed for force/impact con-

trol for both cases i.e, with/without passive damper using a commercial package of MATRIX$_X$ [3] to discuss the effect of passive damper on system stability.

3.1 Force Control

One of the simple methods to determine the system stability is the root locus plot. For the simple proportional force controller, small values of K_{fp} were observed for both environments [9]. Large value of K_{fp} above the marginal value can destabilize the system, so the K_{fp} should be small to guarantee stable contact. As a result, the system response may be sluggish. We use the integral force compensation method to improve the force control performance. The ZOH[3] effect modifies the open-loop dynamics as follows:

$$G_{op}(z) = K_{fi} G_c(z) G_p(z) , \qquad (10)$$

where $G_{op}(z)$ = open-loop system dynamics in z-domain,
$G_c(z) = \frac{T}{2}\frac{(z+1)}{(z-1)}$
= discrete integral controller with unit gain,
$G_p(z) = \frac{z-1}{z}\mathcal{Z}\{\frac{G_p(s)}{s}\}$
= discretized plant dynamics.

Fig. 4 shows the root locus plots for the both environments based on Eqn. (10) when the passive damper is not considered and the sampling rate is assumed as 700.0Hz. The marginally stable gain values of K_{fi} were about 123.0 for rubber plate and 785.0 for the steel ingot. These values are very larger than those for proportional force control. Those, however, have nothing to do with the passive damper because the analyses was confined to get the marginal gains for both environments without passive damper. Although it is not as rigorous as the above analyses, the effect of passive damper will be discussed in the next section for impact control where the passive damper is required seriously.

Before we go into further analysis of passive damper, it is worthwhile to point out the limitations of active damping method for force and impact control. One of the interesting facts is that the use of active damping can not reduce the contact force level for high stiff environment and can not stabilize the system. In our case, the reason can be explained as follows when the steel ingot is considered as the environment. The total system stiffness is

$$K_{as}' = \frac{K_s K_a}{K_s + K_a} \simeq 0.846\,\mathrm{MN/m} , \qquad (11)$$

and the minimum resolution of joint position can be sensed from the joint position sensor is

$$\theta_{min} = \frac{2\pi}{65536} \simeq 96.0\mu\mathrm{rad} . \qquad (12)$$

Considering the arm length is 0.25m, the minimum force level which can change the joint position is above about 20.0N. If the force is below this value, the measured joint position does not change essentially because of the high stiffness of the environment. As a result, the computed joint velocity is zero and the active damping gain has no effect on the system response. This is the typical phenomenon when the arm is to exert desired force to the high stiff environment. This is the limitations on fine force control when the environment is highly stiff as steel ingot. To control fine force for those stiff environment, one need expensive position sensor with high resolution to resolve this problem.

3.2 Impact Control

We use the impact controller as a combination of PID position controller and the explicit force controller. The switching of control modes between position/force is determined by measuring the force. The block diagram of the impact controller is shown in Fig. 5, where the switching variable S is set to 1 for the position control mode. As soon as the measured force is over a prescribed threshold force value, then it is set to 0. When the passive damper is attached, then the solenoid valve will be operated at the same time. Fig. 6 is the simulation result of the impact control to show the effect of the passive damper to the system stability. Fig. 6(a) is the result when the use of passive damper is not considered and Fig. 6(b) is obtained when the passive damper is used. As the force control law, the PI force compensation method with velocity feedback is assumed. The control parameters are given by the same values for both cases. The K_{fp} is 0.15, the K_{fi} is 20.0 and the K_{fv} is 20.0. The environment is assumed as the rigid body and the desired contact force is 15.0N. One of the obvious facts is that the system stability can be improved by using the passive damper. This can be interpreted as follows: the active damping gain K_{fv} can not be increased largely enough because of the noise effect which is generated from the numerical differentiation and the large damping gain can unnecessarily excite the system dynamics. However, the passive damper can provide neat natural damping characteristic of the system, so it can contribute really to the system stability. This result will be verified via experiments in the next section.

4 Experiments

The experimental device is the 1-DOF direct-drive arm moving in the vertical plane. The motor is driven by PWM amplifier which uses the inner current loop. Joint position is measured by a 16-bit absolute type of encoder and joint velocity is computed by numerical differentiation. An IBM-PC/AT is used as a main controller. The arm is equipped with an one-axis force sensor at the tip and to reduce noise effect, a RC-passive low-pass filter is employed. In all experiments, the sampling rate is fixed as 700.0Hz.

4.1 Force Control Performance

[3]ZOH means the zero order hold

As the force control strategy, the integral force control method is employed based on the previous analyses. Initially, the arm maintains in contact with the environment and we add some velocity feedback gain to improve the force control performance. In this situation, there is no excessive impact force to the arm, so the effect of passive damper is not so significant. When the passive damper is used, we do not add the active damping because the passive damper itself has enough damping characteristic. But when a high integral gain is used, some active damping was used to get better performance especially for transient period, where the passive damper is not activated during that time. For soft rubber plate, the integral force control technique with active damping method can improve the force control performance [9]. For the steel ingot environment, however, the active damping method is not effective because of the limitation of the position sensor as described before. Fig. 7 shows the experimental results, where the integral gain K_{fi} is chosen as 80.0 in both cases and the velocity feedback gain K_{fv} of 30.0 is added in Fig. 7(b). In both cases, 20.0N of the desired force is commanded. As expected, the system responses show almost the same results even the active damping is added for Fig. 7(b). Specially, in dealing with impact, we can not increase the active damping gain arbitrarily large to get stable contact and high value of the gain can destabilize the system especially for high stiffness environment. This point justifies the use of the passive damper.

4.2 Impact Control Performance

For all impact experiments, the approaching speed is about 0.26m/s at the tip of arm. In dealing with the impact, the initial high force spike may be inevitable. But, after rebounding due to the initial collision, the re-approaching velocity to the initial contact point must be reduced to prevent the successive collisions. This may be easily accomplished for soft environment such as rubber by adjusting the velocity feedback gain K_{fv}. For the soft rubber plate, whether the passive damper is attached or not, it is easy to make the stable contact without large impulsive force except the initial force spike [9]. For the steel ingot, however, the quantizing effect of joint position sensor affects seriously on stable contact. The worst case can be illustrated in Fig. 8 where the active damping can even make the system unstable specially for high stiff environment. Fig. 8 shows experimental results on this fact when the passive damper is not used where the integral force feedback gain K_{fi} is given by 5.0 in both cases. The velocity feedback gain K_{fv} is given by 25.0 for Fig. 8(a) where the response is unstable, and 15.0 for Fig. 8(b). Even if we can get stable contact for small K_{fv} without passive damper, the peak forces during the initial period is very large near 120.0N. This result also drastically shows the limitations on the magnitude of active damping and verifies the previous analysis. When the passive damper is attached, we can now increase the K_{fi} and K_{fv} to produce good responses. When we use the integral force control only, it is possible to use high integral force feedback gain of even 80.0 and higher integral force feedback gain produces faster restoring time to the contact point after the initial collision.

To show the critical effect of the passive damper and to verify the simulation result of Fig. 6, more severe case was considered. We change the force control law as PI force control method. This will produce fast response but the added proportional force feedback gain K_{fp} can destabilize the system as mentioned in the previous force control analyses. The experiments were performed for the same conditions except the attachment of the passive damper and Fig. 9 shows the experimental results. The steel ingot was used as the environment and K_{fp} was given by 0.20, K_{fi} and K_{fv} were given by 20.0 respectively in both cases. Firstly, we can notice that the results of Fig. 6 and Fig. 9 match well. As experimentally shown in this figure, when the passive damper is not attached (refer to Fig. 9(a)), the system is unstable and successive collisions are happened. While the passive damper is used (refer to Fig. 9(b)), the contact force level is below 50.0N and it takes about 0.14s to achieve the stable contact. Note, also, that the force level was over 100.0N and the time to achieve stable contact was over 0.25s for Fig. 8 without passive damper. From the figures, we understand that the passive damper can reduce the contact force except the initial impact and can increase the stable boundary of the system. This result is somewhat expected as the passive damper can generate large natural damping and this produces reduced re-approaching velocity after the initial collision. Also, in steady state, it can be observed that the force controller works well to exert desired force as shown in these figures.

5 Conclusion

As a way to handle the force and impact control problem, the newly developed passive damping method was proposed. The modeling of the system for force and impact controls was performed.

As the force control strategy, the integral force control method shows satisfying result through the analysis and experiments. It was also pointed out that when the joint position sensor is used for the velocity estimation, the active damping method was not effective to produce damping characteristic to the system especially for stiff environment.

Impact control experiments were performed using PID position control and the explicit force control method for the low/high stiff environment. For hard environment, however, the velocity feedback could not add the damping characteristics after the arm contacts with the environment. Also, it was shown that large value of velocity feedback can even destabilize the system. The system stability was shown to be improved and the amount of

contact force level after initial collision could be reduced using the passive damper while performing good force tracking capabilities.

References

[1] K. Youcef-Toumi, and D. A. Gutz, "Impact and Force Control", IEEE Int. Conf. on Robotics and Automation, pp. 410-416, 1989

[2] L. S. Wilfinger, J. Wen, and S. Murphy, "Integral Force Control with Robustness Enhancement", IEEE Int. Conf. on Robotics and Automation, pp. 100-105, 1993

[3] "MATRIX$_X$ User's Guide", Integrated Systems Inc., 1990

[4] N. Hogan, "Stable Execution of Contact Tasks Using Impedance Control", IEEE Int. Conf. on Robotics and Automation, pp. 1047-1054, 1987

[5] O. Khatib, and J. Burdick, "Motion and Force Control of Robot Manipulators", IEEE Int. Conf. on Robotics and Automation, pp. 1381-1386, 1986

[6] R. A. Volpe, "Real and Artificial Forces in the Control of Manipulators: Theory and Experiments", Ph.D Thesis, CMU, Sep., 1990

[7] S. D. Eppinger, "Modeling Robot Dynamics Performance for Endpoint Force Control", Ph.D Thesis, MIT, Sep., 1988

[8] Y. F. Zheng, and H. Hemami, "Mathematical Modeling of a Robot Collision with its Environment", Journal of Robotic Systems, 2(3), pp. 289-307, 1985

[9] Y. H. Oh, "Robot System Modeling for Force and Impact Control", MS Thesis, POSTECH; Feb., 1993

[10] Y. M. Kim, "Impact Control of Direct Drive Manipulator Using Passive Damper", MS Thesis, POSTECH, Feb., 1992

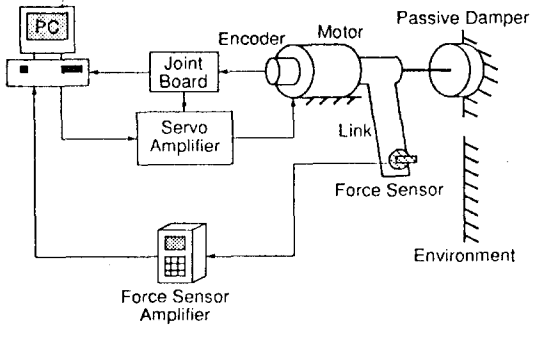

Figure 1: Schematic diagram of the System

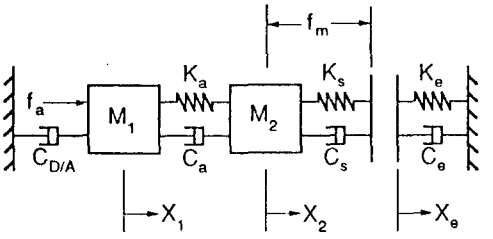

Figure 2: Force controlled system model

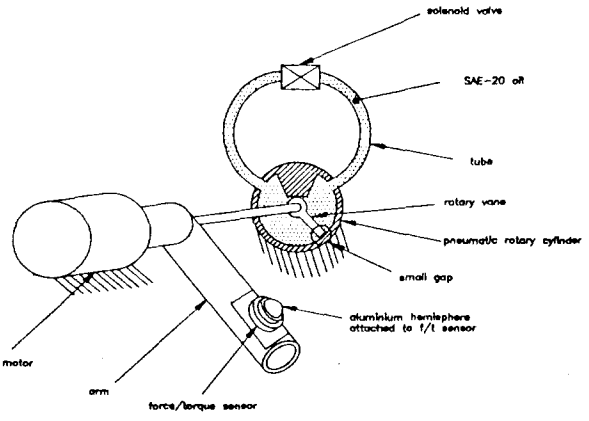

(a) Schematic diagram

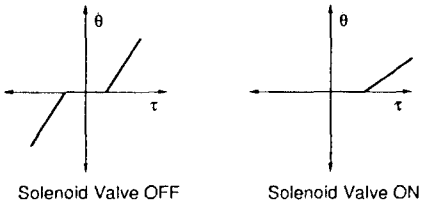

(b) Ideal characteristic

Figure 3: Schematic diagram and characteristic of the passive damper

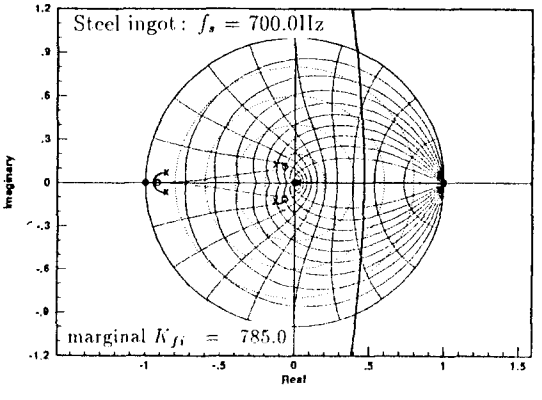

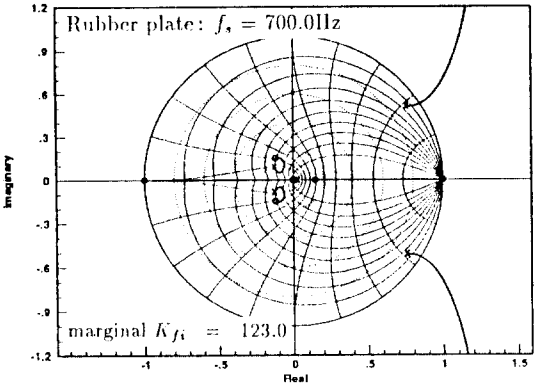

Figure 4: Root locus plots in discrete domain: K_{fi} as a parameter, without passive damper

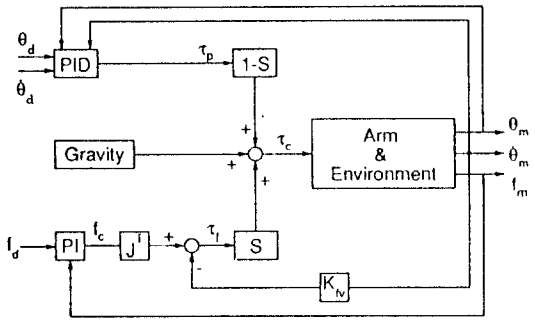

Figure 5: Schematic diagram of the impact controller

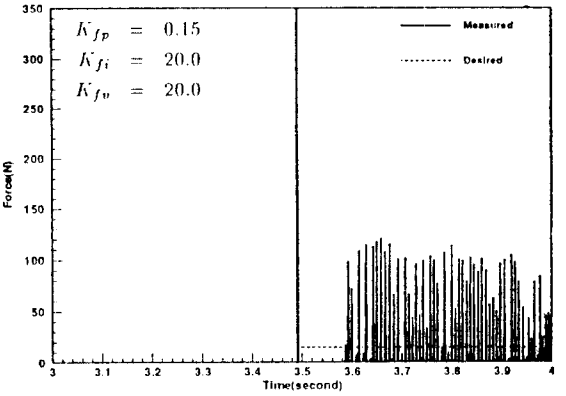

(a) Without passive damper

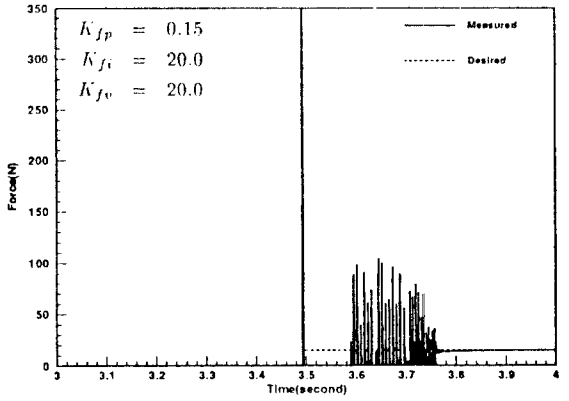

(b) With passive damper

Figure 6: Simulation results of impact control for steel ingot

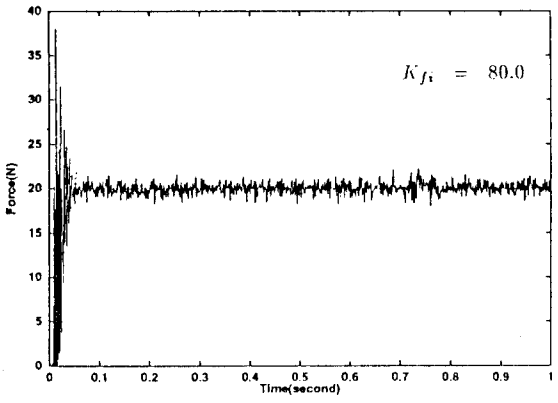

(a) Without active damping

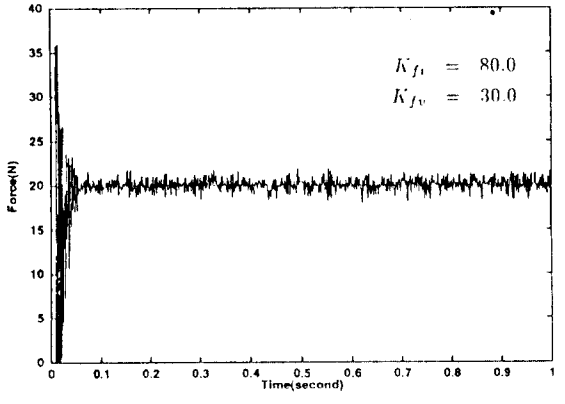

(b) With active damping

Figure 7: Integral force control experiment for steel ingot with passive damper

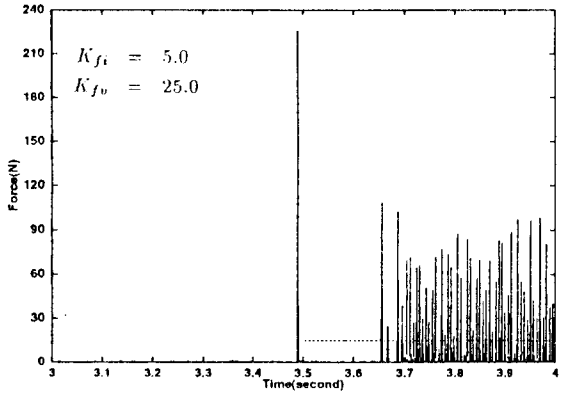

(a) Active damping: $K_{fv} = 25.0$

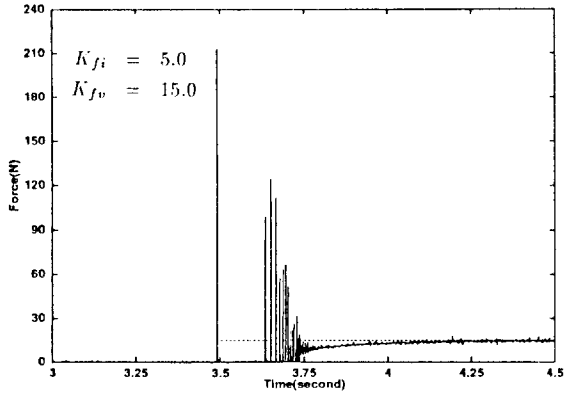

(b) Active damping: $K_{fv} = 15.0$

Figure 8: Impact control experiment for steel ingot without passive damper: limitations of active damping method

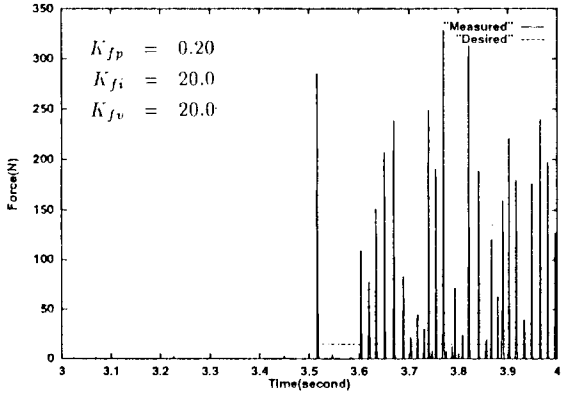

(a) Without passive damper

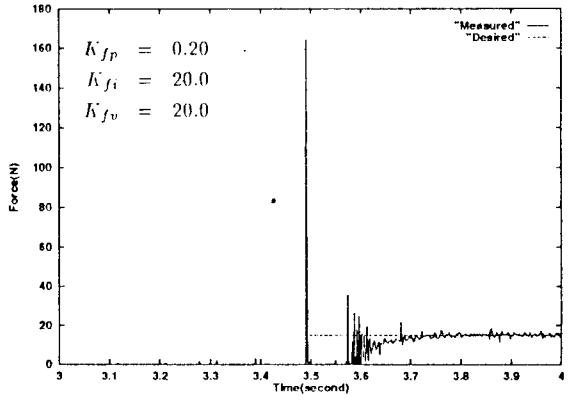

(b) With passive damper

Figure 9: Impact control experiment for steel ingot to show the effect of passive damper